International Journal of Research Publication and Reviews

Journal homepage: www.ijrpr.com ISSN 2582-7421

An Improved Brain Tumor Detection and Segmentation Framework Using Deep Learning Methodology

Sathiya Girija H[a], Indhuja Nivetha H[b], Dhanalashmi K[c], Atheshwaran K[d], Bharath S[e]*

a Assistant Professor, Dr.Mahalingam College of Engineering and Technology, Pollachi – 642 003, India.
b UG Scholar, Sri Eshwar College of Engineering, Coimbatore – 641 202, India
c UG Scholar, Sri Eshwar College of Engineering, Coimbatore – 641 202, India
d UG Scholar, Sri Eshwar College of Engineering, Coimbatore – 641 202, India
e UG Scholar, Sri Eshwar College of Engineering, Coimbatore – 641 202, India

A B S T R A C T

Using deep learning strategies has a substantial effect to forecast tumor presence when it comes to clinical image segmentation on brain MR images. Handson segmentation of a brain tumor is a complex process as it depends on expertise and experience of medical professionals. In this paper, we provide a semantic segmentation approach by using convolutional semantic network to instantly sector brain tumor on 3D Brain Tumor Segmentation (BraTS) image data sets. This consist of 4 various imaging modalities (T1, T1C, Flair, and T2). Additionally, our research study consists of 3D imaging of the entire brain and contrast between ground fact and forecasted labels in 3D. To acquire specific growth area and measurements such as depth, size as well as height, this technique was used efficiently and images were presented with various planes consisting of sagittal, axial and coronal. Assessment outcomes of semantic segmentation which was implemented by a deep learning network are considerably appealing about tumor prediction. The mean prediction ratio was established as 91.718. Mean IoU (Intersection over Union) as well as Mean BF rating were computed as 86.946 and 92.938, specifically. Dice ratings of the examination images were revealed to have considerable resemblance between ground reality and anticipated labels. Therefore, both semantic segmentation metrics and also 3D imaging can be taken purposefully for identifying brain tumor properly.

Keywords: Deep learning, tumour diagnosis, brain MR images, BraTS imaging, semantic segmentation, 3D imaging.

1. Introduction

A brain tumor can be either a non-cancerous or malignant development of unusual cells in the brain, which can be referred to as benign or malignant. The benign lumps remain in a framework of harmony as well as exclude active cells, whereas malignant lumps include energetic cancer cells, which have a non-uniformity structure [1, 2]. These growths can be categorized as main brain tumors and metastatic ones. In main brain tumors, the cells are essentially brain cells, nevertheless, in metastatic tumors, cells with cancer cells have spread out right into the brain from one more body component which is contaminated. The important sort of tumor is called gliomas and also, they can be varied from state-of-the-art (HG) growth called glioblastoma multiform (GBM) to low-grade (LG) lumps like astrocytomas or oligodendrogliomas [3, 4].

Detecting brain tumors from MRI (Magnetic Resonance Imaging) images by using software-based applications consist of procedures such as segmentation, growth discovery, and classification. To identify brain tumors with greater precision and credibility, the application of deep learning approaches has actually been an area of substantial possibility and assurance [5]. The major function of identifying brain tumor with computer-aided systems is to get considerable professional info relating to the tumor kind, visibility, and location [6].

Segmentation of MRI brain image data has exceptional advantages on the software-based clinical image evaluation to identify tumors much more accurately. MRI images can be dramatically impacted by noise and artifacts, which trigger a much harder segmentation procedure, due to the restriction of image acquisition tools [7]. Although MRI is a reliable strategy to define brain framework precisely, criteria such as inadequate spatial resolution, reduced

* *Corresponding author.*
E-mail address: sathya11.sece@gmail.com

comparison, inhomogeneity and instability of item forms can make clinical image segmentation trivial [8,9,10). In computer-aided clinical image evaluation and medical diagnosis, segmentation is reliable and dependable pre-processing technique. MRI brain images have a large range of applications because of their complicated physiological framework and value for exploring human habits. The non-uniformity, which is brought on by radio-frequency coil develops an extra difficult segmentation procedure because of the unclear framework of the cell borders on the image [11,12].

In literature, there exist numerous computer-aided methods for medical image segmentation, such as fuzzy-based, semantic-based, artificial neural network (ANN) [13, 14]. According to current research, a convolutional neural network (CNN), which is among the deep learning approaches is fairly valuable segmentation process because of its capability to facilitate high precision [15,16]. Deep learning is carried out by a convolutional multi-layer neural network as well as its design comprises several complimentary parameters and hidden layers. With this methodology, each MRI input image relocates through a set of convolution layers, merging layer, filters/kernels, and fully-connected layers and also in the last phase, a process is conducted for the output generation procedure [17].

Numerous kinds of deep knowing network frameworks, as an example, CNN, consist of deep residual Network (DRN), deep feed-forward network, deep convolutional neural network (DCNN) and also U-Net. Amongst these deep knowing strategies, the CNN is one of the most usual one in the area of the image handling because of its special framework. This framework entails an input layer, function removal lavers that collaborate with convolutional layers, a rectified linear unit (ReLU) layer to trigger the feature, merging layers, as well as category layers [17]. Recently, CNN came to be a preferred technique to examine medical images. To use the division with CNN, target voxel or pixel is authorized with a patch and afterward fed right into networks as input and also for the result of the networks; the facility voxel can be used. Because of the convolutional layers, CNNs record substantial non-linear matching between outcomes and inputs [18-20]. CNN can determine complicated features from the brain images. For the inputs of CNN, spots of MRI brain images were removed and are fed right into the network for processing. Furthermore, to remove these complicated features, trainable convolutional filters and also local subsampling are used [21, 22].

Restoration of three-dimensional medical images has an increasing interest in the biomedical research studies. To restore such data sets right into 3D volumes via recording of 2D slices, there are numerous kinds of applications [23-25]. For this idea, one research study recommends an updated approach for automated option of landmarks along the contours of 2D MRI slices of the human brain. To carry out automated segmentation, the needed formulas can be categorized as landmarks and non-landmark based techniques [23].

The manual segmentation of 3D MRI images performed by medical professionals depends upon the practical knowledge and experience of the medical professional. To avoid user-based breakdowns in addition to problems stated prior in this paper, automated segmentation algorithms can be applied on medical images given that they can offer dependable and quantifiable outcomes. Due to the reduced contrast between soft cells, enhanced noise, as well as various kinds of artifacts in MRI images, can mitigate precision while identifying and can cause misdiagnosis [26, 27]. The automatic brain-image segmentation process can be classified right into 3 courses such as statistical-based, learning-based, and atlas-based, which was explained previously. Amongst these 3 groups, learning-based strategies are one of the most reliable ones given that they do not need the registration step. Rather, they use obtained features from qualified images for the function of learning a monitored segmentation version [28, 29]. To eliminate the restrictions of using hands-on functions, the deep learning technique of deep convolutional neural networks (DCNNs) was created, which has considerable significance on brain image segmentation [30, 31].

In general, 3D MRI image data are adopted because it can be valuable to make a DCNN to perform 3D volumetric segmentation. The network can offer spatial details amongst adjacent image cuts [26]. To use segmentation effectively to three-dimensional clinical images by using deep learning approaches, there are various kinds of concerns such as the background of the clinical images, restrictions of source memory and unpredictable dataset issue [32]. This particular research suggests various methods relating to the segmentation of 3D clinical images by using a deep learning network. It is called ' Multi-projection' network, which safeguards the memory of sources by using 2D kernels as getting the 3D details of the image by merging slices which are obtained at various planar projections [32]. As an input brain image, BRATS datasets were used which have 4 various techniques for every brain image. These can be identified specifically as T1 (native), T1C (post-contrast T1-weighted), T2 (T2-weighted) and Flair (T2 Fluid Attenuated Inversion Recovery) [33]. One more research study offers various techniques which can be specified as a brand-new two-stage fuzzy multi-objective structure in order to segment 3D MRI brain images in the existence of high noise and inhomogeneity density. This formula includes 2 phases as complies; a) 3D Spatial Fuzzy C-Means (3DSpFCM) and also b) 3D Modified Fuzzy C-Means (3DMFCM) [7] As necessary, the UNet and 3D-UNet are also extremely typical CNN applications for clinical image evaluation. The framework of the UNet includes encoder-decoder; low level attributes are found by encoder component while top-level features are found out by the decoder with the features acquired from an encoder. This design can be called an end-to-end network and can create substantial outcomes in medical image segmentation [34, 35].

In our work, it is intended to introduce a different segmentation approach on MRI brain images by using one of the CNN methods, which are formerly discussed. By using CNN, it is meant to raise the precision of growth medical diagnosis as a lot as feasible. While executing this procedure, an additional essential objective of the research study is to develop a 3D brain model with malignant growth. Furthermore, the procedure intends to draw out the lump framework in the 3D version to supply details on measurements of the tumor concerning deepness, height, size for figuring out the specific location of the deadly tumor. As a dataset, BRATS image information, which consists of MRI brain image on 4 various methods, was used.

2. Literature Survey

Image segmentation is one of the most sought after a medical image processing method which is widely preferred for the diagnosis of brain tumors in recent times. Although there are several studies regarding brain tumor segmentation, it is still difficult job to draw out a specific tumor structure without increasing the complexity. Even with substantial growth in the field of heath applications, the development of a 3D design model of the brain and the tumor itself poses a huge challenge to the researchers. Hereof, we evaluate some pertinent studies concerning brain tumor segmentation [36-40].

In the first suggested research, for the function of identifying brain tumors with automated segmentation such as necrosis, edema and growing tumor, a convolutional neural network SegNet was used to 3D information collections for 4 various MRI modalities consisting of T1, T1ce, Flair as well as T2. To boost tumor segmentation also much better, SegNet versions are trained independently were incorporated with post processing procedure. After this component, a decision tree strategy was used to classify MRI voxels for identifying various tumor components and healthy brain cells. The recommended algorithm resulted in three various F-measure scores of 0.85, 0.81, and 0.79 for entire growth, tumor core and expanding growth; specifically [36].

One more research study recommends a deep learning system for tumor segmentation and estimate of the survival rate in glioma by using various MRI modalities. For using tumor division, 3 various 3D CNN architectures were used to boost the efficiency of the network. For survival evaluation, 4.524 radiomic features were removed from segmented tumor areas, afterward, a decision tree and cross validation strategies were used. With this offered design, 61.0% precision was attained on the classification of short-survivors, lengthy, and mid survivors, respectively [37].

Various other provided researches offer a 3D U-Net architecture which can be used for segmentation of radiologically recognizable sub-regions such as edema, necrosis and also developing tumors. To stress the problem of class discrepancy between tumor and non-tumorous patches, a system which is composed weighted patch from the lump border areas existed. This specific framework includes a contracting path to acquire details about context and symmetrical broadening course that permits precise localization. The Deep Convolutional Neural Network (DCNN) was used to train 285 MRI images, confirms 66 sick persons and checked on 191 sick people. Dice scores of this suggested model are specifically 0.88, 0.83 and 0.75 for the entire tumor, growth core, and progressing tumor [38].

The objective of an additional research was to improve classification accuracy while lowering the danger of overfitting issue and to facilitate the multi-class classification. The system consists of a CNN with enhanced softmax loss function and regularization. According to the outcomes of this research, the suggested version has a far better precision by 2% and reduced handling time of 40-50 ms compared to various other present systems. This version likewise comes with issues like binary classification, the computation time and the overfitting of the information [39].

The last evaluated technique uses a deep CNN as well as combines unique segmentation as well as error improvement sections. In this research, segmentation masks were created to run with orthogonal slices of the input information as well as failure labels are later fixed by a gathering of Replace and Refine networks. Outcomes of this technique have a mean Dice value of 0.9015 while the needed segmentation time for MRI volume was 14.8 s [40].

Our research study varies from these associated research studies by using semantic segmentation, which uses deep learning network for a procedure of 3D imaging of the tumor area.

3. Proposed Methodology

3.1. Image data set description

In this research, we use BraTS dataset to review the segmentation efficiency of our recommended technique. Brain MR dataset has 257 training images with matching labels and the dimensions of these MR photos are 240 * 240 with 155 slices and 4 various imaging modalities consisting of T1 (T1-weighted), T1C (contrast boosted T1-weighted), T2 (T2-weighted), as well as FLAIR (Fluid Attenuation Inversion Recovery). As test images, 5 various MR images were used to use semantic segmentation for history and tumor forecast as well as assess segmentation metrics such as mean accuracy, imply WeighteIoU, meanbfscore as well as iou [49] The experiment was performed on a computer system with i7 9th generation processor device at 2.60 GHz/8GB RAM and NVIDIA GEFORCE GTX. Each magnetic resonance imaging modalities interpret detecting brain tumor. T2 images are used to figure out edema tumor areas, healthier cells can be identified on T1 images, T1C imaging modality can be related to identify the lump boundaries and edema areas can likewise be differentiated from cerebrospinal fluid on FLAIR pictures [41, 42] Our suggested approach uses all imaging modalities, which are first used on pre-processing imaging application before they fed right into neural network as an input image. After these MR images were presented on MATLAB, some picture processing methods such as image sharpening and histogram equalization were used on initial images to boost the contrast. These procedures can be seen in Fig. 1. All slices can likewise be displayed in Fig. 2.

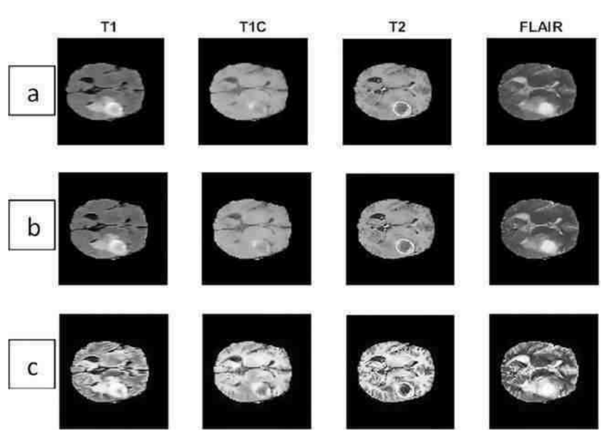

Fig. 1. Various types of MR modalities and pre-processing operations a) original images, b) Sharpened images, c) images with histogram equalization.

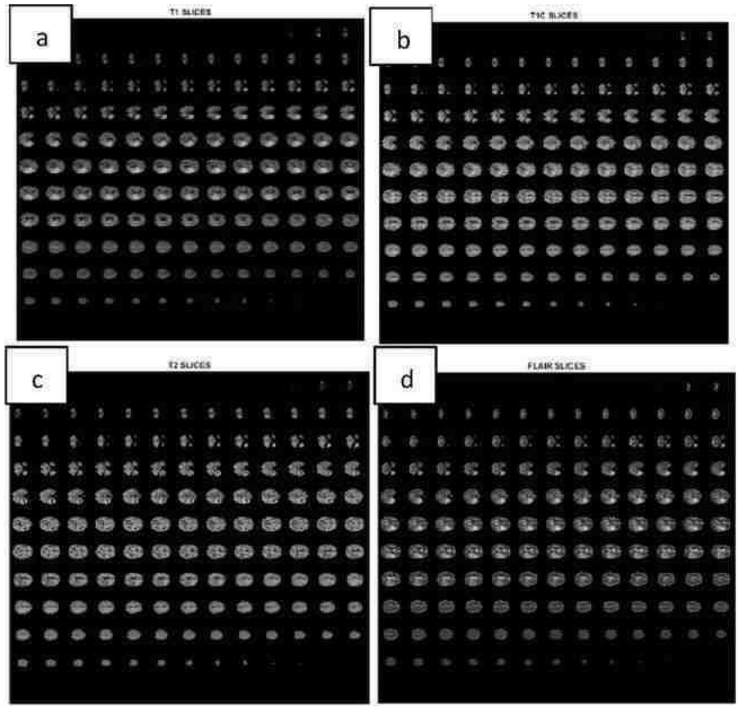

Fig. 2. Summary of MR images with four different modalities a) T1, b) T1C, c) T2 and d) FLAIR.

Our recommended system begins with image procurement on MATLAB modeled on by pre-processing application, which is mentioned earlier, such as histogram equalization. Random patches are obtained from MR images are fed right into neural network as an input. The training procedure of this network, which is composed 16 layers such as convolution layers, batch normalization layers, relu layers, max-pooling layers representing down-sampling as well as for up-sampling, shifted convolution layers and relu layers were used. Deep learning network is finished with softmax layer and pixel classification layer. After training procedure, test images were used to use semantic segmentation.

Outcomes of semantic segmentation consist of segmented MR slices and predicted labels. In the last stage, semantic segmentation outcomes exist and 3D imaging consisting of the entire brain, ground reality and anticipated labels and tumor region. The block diagram and flowchart of our suggested technique are displayed in Figs. 3 as well as 4.

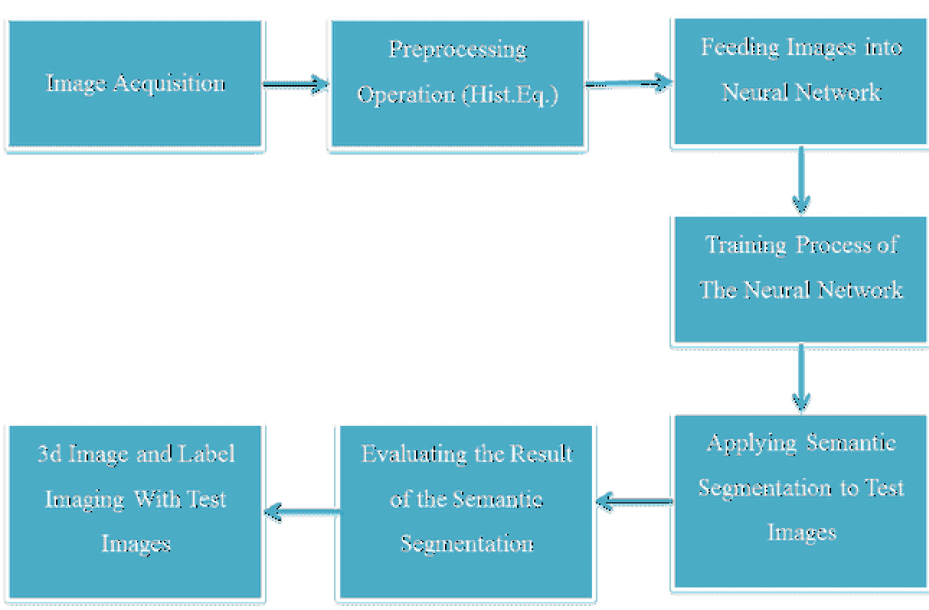

Fig. 3. Schematic overview of the proposed framework.

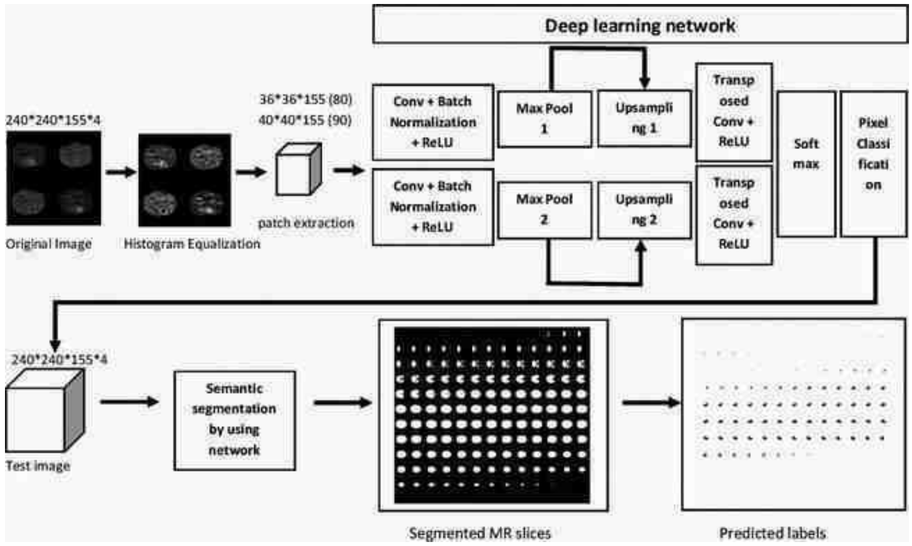

Fig. 4. Overall block diagram of deep learning network and semantic segmentation process.

3.2. Pre-processing

As it is displayed in Fig. 4, histogram equalization was employed to authentic images to improve the contrast. We used flexible histogram equalization strategy, which uses a much method than routine histogram equalization by calculating numerous histograms. Each of these histograms matches a unique section of the photo and uses them for rearranging the lightness worth of the image. This technique offers renovation of the local contrast as well as improves the meanings of the sides in each area [43] Hereafter area; arbitrary patches are drawn out alike from 2 image based data store consisting of network inputs and wanted network feedback for training. It can likewise be used for ground truth images as well as pixel tag information for the function of training semantic division networks. Dimensions of the patches are changed as 36 * 36 * 155 and 40 * 40 * 155 as well as the variety of spots per picture are 80 and 90, specifically. Because there were some memory problems, factor for choosing these spot dimensions is to maximize the deep knowing network as well as enhance the efficiency of the network as a lot as feasible. After performing numerous experiments, spot sizes with these dimensions have the ideal result.

3.3. Deep learning network

Our recommended deep learning network essentially is composed down sampling and up sampling procedures which were used by convolution and transposed convolution layers. Semantic segmentation was put on check images by using the network whose streamlined framework is received as shown in Fig. 5. Extracted spots are fed right into deep learning network as an input image. Convolution layers are employed to images that have 12 filters with dimensions of 4 * 4 * 4. This process leads to high efficiency outcomes which can be acquired after some experimental procedure. Thinking about the tumor dimensions, it was intended to implement even more comprehensive evaluation. To accomplish down-sampling procedure, 3D max-pooling layer was used by dividing 3D picture right into cuboidal regions.

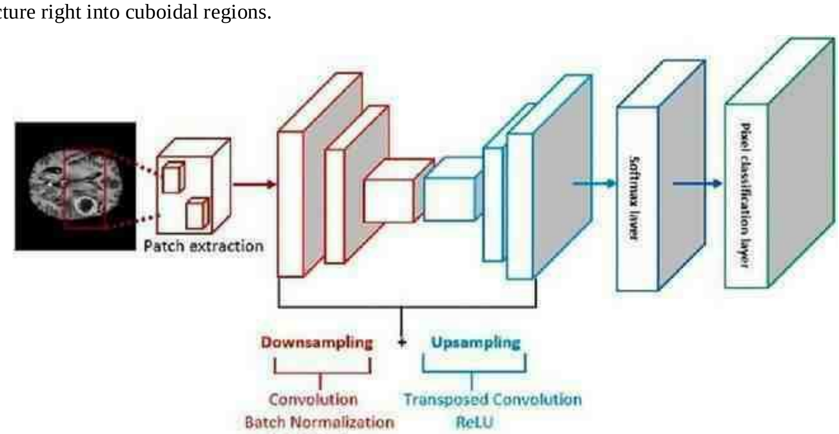

Fig. 5. Overview of the deep learning network adopted for this study.

3.3.1 Down Sampling

Max-pooling layers, which are placed right into network after convolution, batch normalization and relu layers are generally in charge of finishing down-sampling of the image. With these layers, it is intended to handle information about a preferable dimension, offering a faster processing time of the image by minimizing dimensions of input information. Also, these layers play a crucial role in lowering the storage size of the information. The formula for convolution layer is shown in Eq. (1). For three-dimensional image (I), there dimensional filters (F) were used [51, 52].

O (i, j, k) = $\sum_m \sum_n \sum_p I\ (m, n, p) F\ (i-m, j-n, k-p)$ (1)

Matrix form in Eq. (1) can be defined as follow: Input matrix size (number of images) x (width (w)) x (height (h) x (depth(d)) where wand h represent the number of convolution filters and d is corresponding to filter depth.

3.3.2 Up Sampling

Transposed convolution layers are included in the neural network for upsampling the 3D feature maps of the information. The size of image can be boosted at the end of these layers. The exact same dimension of filters as in convolution layers was used for deconvolution procedure. The last layer of the deep learning network is the pixel classification layer, which supplies categorical labels for each and every image pixel or voxel to be used for semantic segmentation.

3.3.3 Semantic segmentation

Semantic segmentation determines the procedure of correlating each pixel of a MR brain image with a course label such as background and also additionally tumor. The application of semantic segmentation by using deep learning network identifies every pixel in an image. This procedure winds up with the segmentation of an image by classes [44, 45). Our technique offers a neural network and application of a semantic segmentation on MR images by using this deep learning framework. The usual framework in semantic segmentation networks uses down-sampling of an image between convolutional and ReLU layers and consists of result up-sampling to match the input dimension. After roughly 3-h training procedure per image finished, test images were offered to the network to employ an effective semantic segmentation.

3.3.4 Performance assessment metrics

Outcomes of the segmentation were reviewed with various metrics consisting of global accuracy, mean accuracy, meanIoU, weightediou, dice-index and meanBFscore. One more analysis procedure for pixel category according to class is to produce a confusion matrix [46]. Each row of the confusion matrix stands for the circumstances in a predicted class and also each column stands for the instances in a true class (Table 1).

Table 1 - Class confusion matrix for pixel classification.

		True class	
		P(Background)	**N (Tumor)**
Predicted class	P(Background)	True Positive (TP)	False Positive (FP)
	N (Tumor)	False Negative(FN)	True Negative (TN)

Global precision defines ratio of properly classified pixels to the complete variety of pixels without trust class. The ratio of properly classified pixels versus complete pixels for each and every class is referred to as a mean precision displayed in Eq. (2) [47].

Accuracy = $\frac{(\mathrm{TP}+\mathrm{TN})}{(\mathrm{TP}+\mathrm{TN}+\mathrm{FP}+\mathrm{FN})}$

To assess the semantic segmentation results more precisely, IOU (Intersection over Union) metric can be used, which is also specified as a jaccard index displayed in Eq. (3) as well as Eq. (4) [48]. This is just one of many usual metrics of a semantic segmentation procedure. It can be discussed as a ratio between overlapping areas of segmented images and also ground truth images [48]. This metric can be more suitable when validated with the resemblance of ground truth labels and also predicted labels. The value of this metric diversified between 0 (no overlap) as well as 1 (full overlap).

Jaccard(A,B) = $\frac{(||A \cap B||)}{(||A \cup B||)}$ (3)

Jaccard = IOU = $\frac{(\mathrm{TP})}{(\mathrm{TP}+\mathrm{FP}+\mathrm{FN})}$ (4)

WeightedIoU is the mean IoU value of all classes and it is identified with weighted mean values of various pixels for every class. BF rating shows the resemblance between anticipated contours of each class as well as true contours. To review semantic segmentation outcomes, dice coefficient has a vital function, which is like IoU revealed in Eqs. (3) and (4) [50]. All these metrics can explain significant statistics concerning semantic segmentation and label prediction.

At the last phase of our research study, 3D imaging of the entire brain, ground truth and estimated labels to compare resemblance and tumor structure concerning the dimensions of tumor with respect to depth, height, and size is provided.

4. Simulation Results

In this work, 257 BraTS image information collection was used for training with deep learning network by using semantic segmentation. To use semantic segmentation with deep learning strategy, we utilized training, test as well as validation images for predicting labels as well as comparing them with ground truth labels. After training procedure finished, 5 types of information were established comprising 155 MR slices with tumor. The examination outcomes of our design, which includes numerous semantic segmentation metrics, are depicted in Fig. 6. In terms of using semantic segmentation by using neural network, 2 classes were determined on MR images such as background and tumor. According to end results, the mean tumor prediction was figured out as 91.72 and mean background prediction accuracy was estimated to be 99.75. Various other metrics for 5 images consisting of mean accuracy, weightedloU and meanIoU were figured out as 95.74, 86.95, and 99.42, respectively. MeanBFScore, which is among one of the most crucial metrics was estimated to be 92.94.

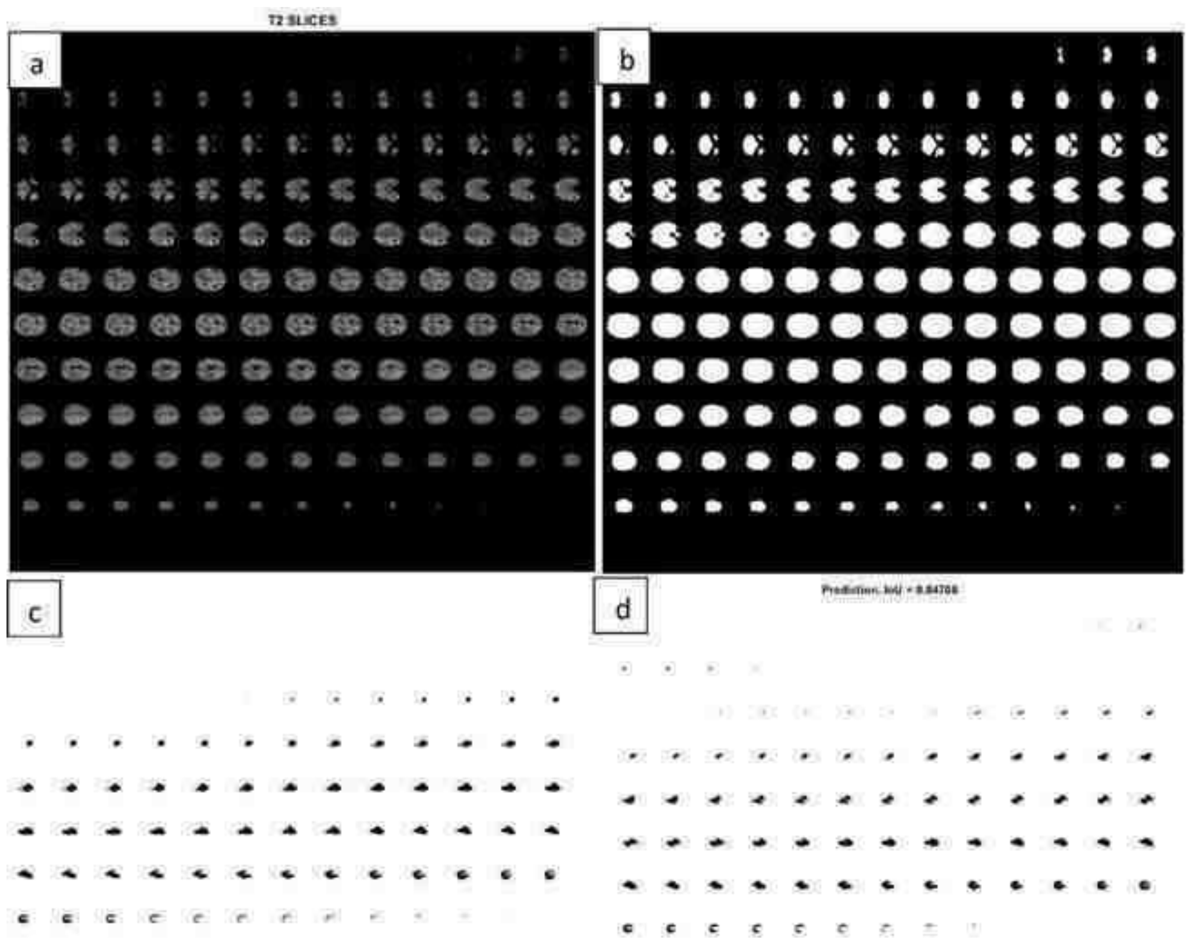

Fig.6. Summary of semantic segmentation results of the first image including ground truth and predicted labels with IoU ratio as 84.71 a) original MR slices (T2), b) segmented MR slices, c) ground truth labels and d) predicted labels.

 International Journal of Research Publication and Reviews Vol (2) Issue (3) (2021) Page 313-324

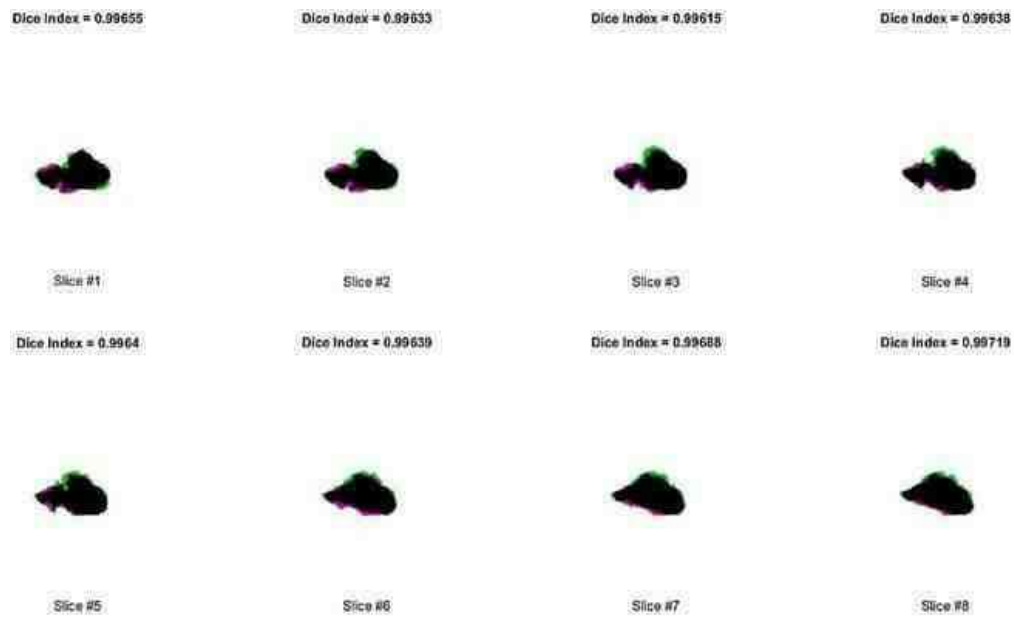

Fig. 7. Similarity index ratios of the first image with dice scores.

3D imaging of the entire brain, ground truth labels and also predicted labels were accomplished on MATLAB by using segmented MR slices as well as labels (Fig. 8). To compare the uniformity between ground truth and prediction, labels were put right into segmented MR slices (Fig. 9) and after that 3D brain model including tumor were acquired to take a look at tumor dimensions extra precisely (Fig. 10).

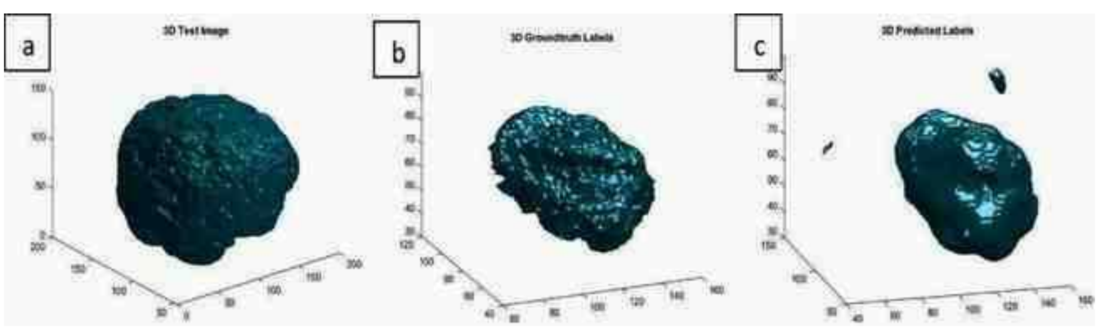

Fig.8. Illustration of 3D imaging by using segmented slices a) whole brain, b) ground truth labels and c) predicted labels (axes represent the pixel number).

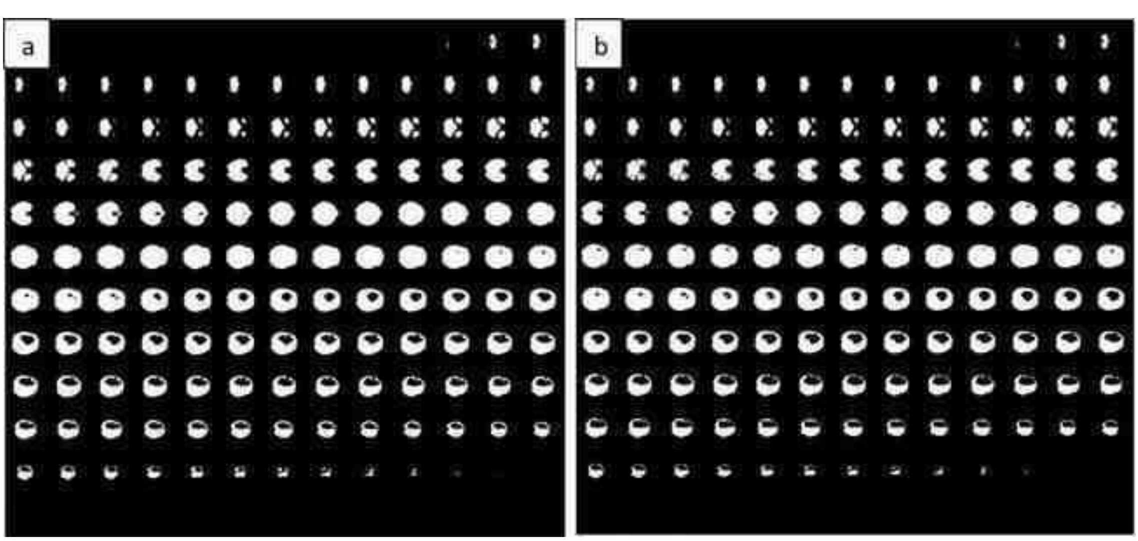

Fig. 9. Process of Label insertion into segmented MR slices, a) MR slices with ground truth labels, b) MR slices with predicted labels.

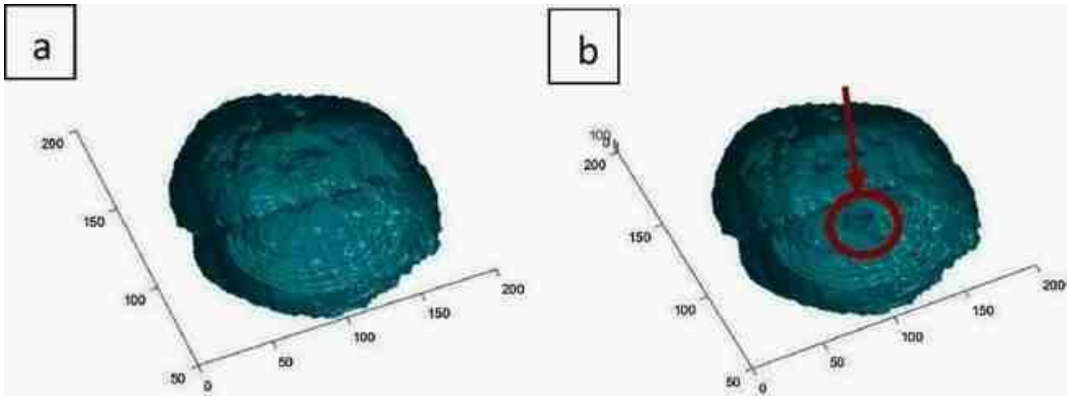

Fig. 10. Overview of 3D MR brain image display using the process of label insertion on to the slices a) ground truth labels, b) predicted labels (axes represent the pixel number)

As a last phase of our research, after ground truth as well as predicted labels put right into segmented images to compare the similarity between these labels as well as 3D models which is produced by utilizing them. To recognize a better specific area of the tumor, 3D versions were created and chopped by using 3D image-cropping feature on MATLAB. These images were presented on 3 various imaging plane consisting of coronal (Fig. 11), sagittal (Fig. 12) and also axial (Fig. 13). They elucidate the tumor area and provide specific details concerning tumor dimensions such as size, depth as well as height.

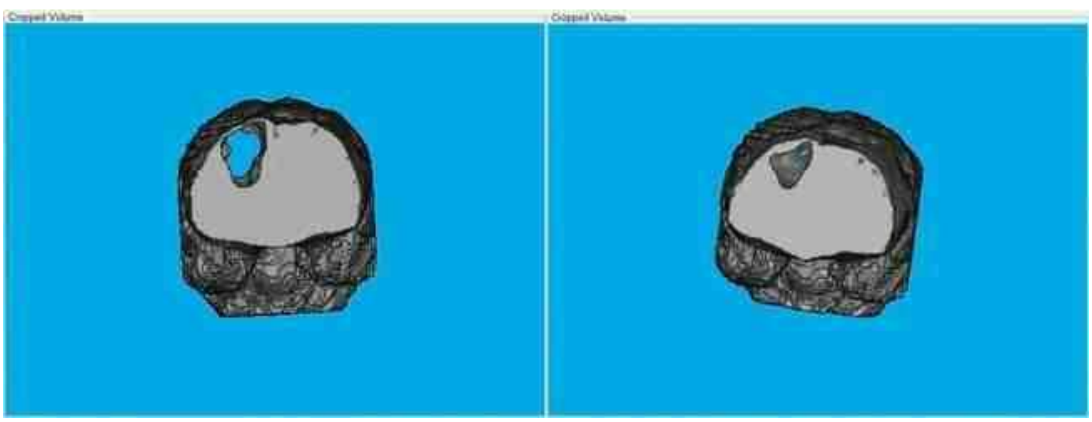

Fig. 11. 3D illustration of precise tumor location on coronal plane.

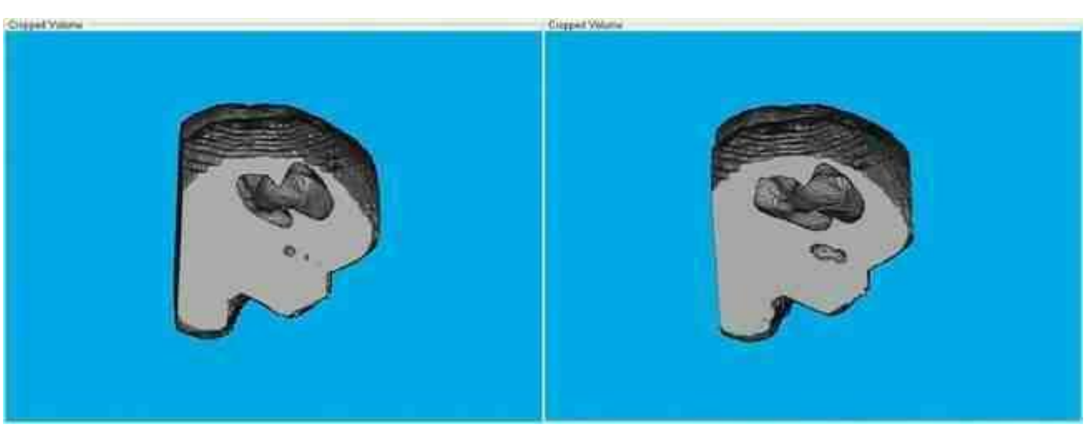

Fig. 12. 3D illustration of precise tumor location on sagittal plane.

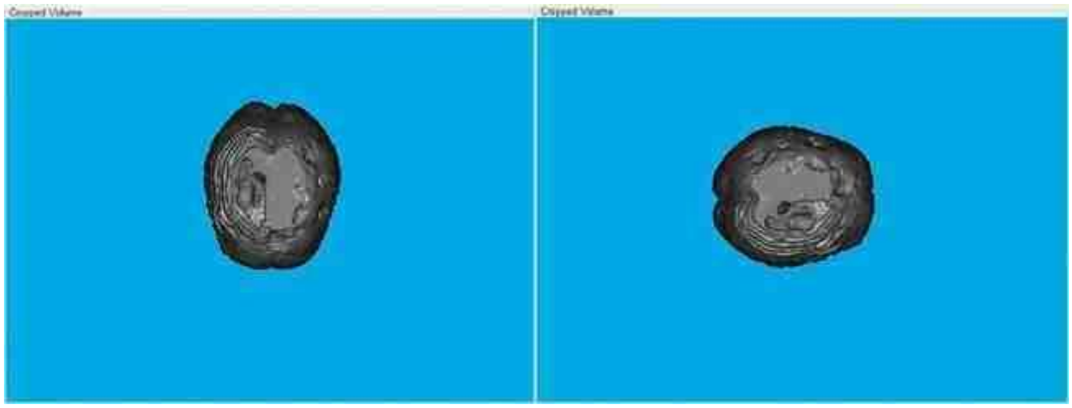

Fig. 13. 3D illustration of precise tumor location on axial plane.

5. Discussions

This paper presents a technique based on semantic segmentation strategy by using convolutional neural network. Our recommended framework uses semantic segmentation on MRI scans to identify background and tumor prediction as well as compare ground truth and predicted labels. 257 MR images with 4 various modalities were trained in deep learning network. After training procedure was effectively finished, 5 various MR examination pictures entailing 155 slices per image were fed right into this neural network for using semantic segmentation procedure. Outcomes of this semantic segmentation network showed substantial values for assessing the segmentation metrics. When our research compared to various other associated jobs, segmentation criteria such as IOU, BF score and dice score exhibit extra trusted and accurate numbers as they were stated previously. Background and tumor prediction were figured out as 99.76 and 91.72, specifically. These proportions can be taken as crucial numbers for assessing the success of semantic segmentation and also getting details relating to the growth area. On the various other hand, for future research studies, our design can be a lot more reliable, when it is performed using even more memory. To eliminate this problem, an external GPU tool can be used, to analyze and evaluate additional test images with much shorter duration. To enhance the pixel classification, patch size and patch per image variables which are obtained from initial images can be raised. Tumor prediction ratio can be created substantially. One more factor to consider boosting the selection of pixel category is to boost the variety of courses. This strategy exhibits efficiency because it consists of much more test information and even more classes.

The objective of this research study also consists of a 3D imaging of brain, ground truth as well as predicted labels and tumors with the insertion of these labels right into segmented images to have relevant information relating to the precise tumor location. Resemblance ratios between ground truth and predicted labels were determined as 86.95, which provide a notion regarding the accuracy of semantic segmentation. To develop 3D brain model comprising tumors, all 155 MR slices were used and superposed. Distinctions between 3D brain models with ground truth labels and 3D predicted labels can be observed in images mentioned previously. This proposed method is an effective technique given that it provides relevant information concerning the precise area of growth concerning depth, size and height.

Table 2 - Comparison between proposed method and other related methods.

Studies	Accuracy	F-Score
Alqazzaz et al., 2019	-	0.85
Li Sun et al., 2019	0.61	0.909
Baid et al., 2020	-	0.88
Maharjana et al., 2020	0.98	-
Ataloglou,et al., 2019	-	0.90
Proposed method	0.957	0.92

Through contrasting the outcomes of literature study as well as our recommended research study, it can be plainly seen on Table 2 that our strategy reveals a considerable F-score versus various other techniques. To review our precision proportion, it can be enhanced with even more memory area or by using custom neural network instead of pre-trained network. In enhancement, contrast with many of the associated studies shows high precision as well as F-score proportions concerning growth forecast. Also though we experienced some memory concerns, we acquired these substantial outcomes by evaluating 5 MR brain images. As we previously specified in this paper, our dice index numbers reveal meaningful outcomes in terms of assessing the similarity between the ground reality and predicted labels.

Furthermore, by using semantic segmentation with a deep learning network, we intended to take a look at the entire brain tumor growth. Our examination metrics plainly reveal that we can discover brain tumor growth with high accuracy and precision. Therefore, this enhanced technique can be applied to MR brain images for in depth assessment.

6. Conclusion

In this research study, we offered various techniques to identify entire brain tumors and present the precise growth area in 3D. Although our design is extremely efficient to predict brain tumors in MR images properly, the efficiency of this system can be established by including even more class identifications to have even more details about the type of brain growth as well as additionally enhancing the variety of training as well as test information, it can be acquired extra results to boost tumor diagnosis. Moreover, 3D version of ground truth as well as predicted labels put in the brain can be advantageous for doctors to recognize the precise area and measurements consisting of height, depth and size.

Finally, with the recommended approach, 2 various courses such as 'background" as well as 'tumor' were defined. By using an arbitrary patch extraction technique, images were fed right into deep learning network. While the mean background prediction was identified as 99.675, mean tumor forecast proportion was computed as 91.618. Additionally, various other semantic segmentation metrics consisting of mean precision, mean IoU mean BF rating and dice index were used to do a thorough evaluation. Outcomes of these analysis metrics are rather appealing. For future research, by raising the variety of test images, a lot more exact outcomes can be obtained. 3D imaging of the brain growth was effectively performed. In the enhancement of segmentation outcomes, 3D imaging can supply a large variety of research studies on brain growth evaluation. It can be claimed that our research study is encouraging and reliable in terms of brain growth discovering and imaging.

References

[1] S. Singh and M. J. Ali, “Primary Malignant Epithelial Tumors of the Lacrimal Drainage System: A Major Review,” Orbit, pp. 1-14, Jun. 2020.

[2] N. N. Bayramova, A. E. Protasova, G. A. Raskin, M. S. Sobivchak, and M. I. Yarmolinskaya, “Endometriosis-assEndometriosis-associated ovarian tumors: morphological and immunohistochemical features,” Malignant tumours, vol. 9, no. 2, pp. 12–19, Jun. 2019.

[3] F. Bozkurt and A. Yousef, “Neimark-Sacker bifurcation of a chemotherapy treatment of glioblastoma multiform (GBM),” Advances in Difference Equations, vol. 2019, no. 1, Sep. 2019.

[4] R. V. Lukas "Commentary: Long-Term Outcomes of Intra-Arterial Chemotherapy for Progressive or Unresectable Pilocytic Astrocytomas: Case Studies,” Neurosurgery, Feb. 2021.

[5] K. Malczewski, “Magnetic resonance image enhancement using highly sparse input," Magnetic Resonance Imaging, vol. 74, pp. 1-13, Dec. 2020.

[6] J. H. Johnpeter and T. Ponnuchamy, "Computer aided automated detection and classification of brain tumors using CANFIS classification method,” International Journal of Imaging Systems and Technology, vol. 29, no. 4, pp. 431-438, Mar. 2019.

[7] A. Al-Shidaifat, S. Kumar, S. Chakrabartty, and H. Song, “A Conceptual Investigation at the Interface between Wireless Power Devices and CMOS Neuron IC for Retinal Image Acquisition,” Applied Sciences, vol. 10, no. 18, p. 6154, Sep. 2020.

[8] A. G. Christodoulou and S. G. Lingala, “Accelerated Dynamic Magnetic Resonance Imaging Using Learned Representations: A New Frontier in Biomedical Imaging,” IEEE Signal Processing Magazine, vol. 37, no. 1, pp. 83–93, Jan. 2020.

[9] K. Teh, P. Armitage, S. Tesfaye, D. Selvarajah, and I. D. Wilkinson, “Imbalanced learning: Improving classification of diabetic neuropathy from magnetic resonance imaging," PLOS ONE, vol. 15, no. 12, p. e0243907, Dec. 2020.

[10] F. C. Damen, A. Scotti, F. W. Damen, N. Saran, T. Valyi-Nagy, M. Vukelich, and K. Cai, “Multimodal apparent diffusion (MAD) weighted magnetic resonance imaging,” Magnetic Resonance Imaging, vol. 77, pp. 213-233, Apr. 2021.

[11] F. Mouffouk, H. Serrai, S. Bhaduri, R. Achten, M. Seyyedhamzeh, A. A. Husain, A. Alhendal, and M. Zourob, “A New Class of Smart Gadolinium Contrast Agent for Tissue pH Probing Using Magnetic Resonance Imaging," Molecules, vol. 25, no. 7, p. 1513, Mar. 2020.

[12] M. A. Morrison and J. M. Lupo, “7-T Magnetic Resonance Imaging in the Management of Brain Tumors,” Magnetic Resonance Imaging Clinics of North America, vol. 29, no. 1, pp. 83-102, Feb. 2021.

[13] S. Wang, J. Jiang, and X. Lu, “Advances on Tumor Image Segmentation Based on Artificial Neural Network,” Journal of Biosciences and Medicines, vol. 08, no. 07, pp. 55-62, 2020.

[14] S. A. Abdalla, Z. A. Mustafa, and B. A. Abrahim, “Brain Tumor Classification Using Principal Component Analysis and Artificial Neural Network,” Journal of Clinical Engineering, vol. 44, no. 2, pp. 70-75, Apr. 2019.

[15] D. A. Priyadharshini, “Tumor Classification in Osteosarcoma Using Convolutional Neural Network,” International Journal of Psychosocial Rehabilitation, vol. 24, no. 5, pp. 1332–1339, Mar. 2020.

[16] W. Qi, X. Zhang, N. Wang, M. Zhang, and Y. Cen, “A Spectral-Spatial Cascaded 3D Convolutional Neural Network with a Convolutional Long Short-Term Memory Network for Hyperspectral Image Classification,” Remote Sensing, vol. 11, no. 20, p. 2363, Oct. 2019.

[17] Gorji and Kaabouch, “A Deep Learning approach for Diagnosis of Mild Cognitive Impairment Based on MRI Images,” Brain Sciences, vol. 9, no. 9, p. 217, Aug. 2019.

[18] H. Chen, Z. Qin, Y. Ding, L. Tian, and Z. Qin, “Brain tumor segmentation with deep convolutional symmetric neural network,” Neurocomputing, vol. 392, pp. 305-313, Jun. 2020.

[19] W. Dang, Z. Gao, X. Sun, R. Li, Q. Cai, and C. Grebogi, “Multilayer brain network combined with deep convolutional neural network for detecting major depressive disorder," Nonlinear Dynamics, vol. 102, no. 2, pp. 667–677, May 2020.

[20] P. Vakli, R. J. Deák-Meszlényi, T. Auer, and Z. Vidnyánszky, “Predicting Body Mass Index From Structural MRI Brain Images Using a Deep Convolutional Neural Network,” Frontiers in Neuroinformatics, vol. 14, Mar. 2020.

[21] X. Zhang, F. Pan, and L. Zhou, “Brain MRI Intelligent Diagnostic Using an Improved Deep Convolutional Neural Network,” Journal of Medical Imaging and Health Informatics, vol. 11, no. 3, pp. 836-845, Mar. 2021.

[22] F. J. Díaz-Pernas, M. Martínez-Zarzuela, M. Antón-Rodríguez, and D. González Ortega, “A Deep Learning Approach for Brain Tumor Classification and Segmentation Using a Multiscale Convolutional Neural Network,” Healthcare, vol. 9, no. 2, p. 153, Feb. 2021.

[23] T. Kim, J. C. Park, H. M. Gach, J. Chun, and S. Mutic, "Technical Note: Real-time 3D MRI in the presence of motion for MRI-guided radiotherapy: 3D Dynamic keyhole imaging with super-resolution," Medical Physics, vol. 46, no. 10, pp. 4631-4638, Aug. 2019.
[24] Z. Wang, Y. Sun, Q. Shen, and L. Cao, "Dilated 3D Convolutional Neural Networks for Brain MRI Data Classification," IEEE Access, vol. 7, pp. 134388 134398, 2019.
[25] H. Hwang, H. Z. U. Rehman, and S. Lee, "3D U-Net for Skull Stripping in Brain MRI," Applied Sciences, vol. 9, no. 3, p. 569, Feb. 2019.
[26] Y. Zhao, X. Ren, K. Hou, and W. Li, "Recurrent Multi-Fiber Network for 3D MRI Brain Tumor Segmentation," Symmetry, vol. 13, no. 2, p. 320, Feb. 2021.
[27] N. Bergsland, "re: Reliability of 3D Texture Analysis: A Multicenter MRI Study of the Brain," Journal of Magnetic Resonance Imaging, vol. 51, no. 4, pp. 1210-1211, Sep. 2019.
[28] H. Xie, H. Lei, Y. He, and B. Lei, "Deeply supervised full convolution network for HEP-2 specimen image segmentation," Neurocomputing, vol. 351, pp. 77-86, Jul. 2019.
[29] L. Xu, H. Xue, M. Bennamoun, F. Boussaid, and F. Sohel, "Atrous convolutional feature network for weakly supervised semantic segmentation," Neurocomputing, vol. 421, pp. 115-126, Jan. 2021.
[30] A. Kermi, K. Andjouh, and F. Zidane, "Fully automated brain tumour segmentation system in 3D-MRI using symmetry analysis of brain and level sets," IET Image Processing, vol. 12, no. 11, pp. 1964-1971, Nov. 2018.
[31] Y. Ding, R. Acosta, V. Enguix, S. Suffren, J. Ortmann, D. Luck, J. Dolz, and G. A. Lody gensky, "Using Deep Convolutional Neural Networks for Neonatal Brain Image Segmentation," Frontiers in Neuroscience, vol. 14, Mar. 2020.
[32] T. Hassanzadeh, D. Essam, and R. Sarker, "2D to 3D Evolutionary Deep Convolutional Neural Networks for Medical Image Segmentation," IEEE Transactions on Medical Imaging, vol. 40, no. 2, pp. 712-721, Feb. 2021.
[33] F. Kofler, C. Berger, D. Waldmannstetter, J. Lipkova, I. Ezhov, G. Tetteh, J. Kirschke, C. Zimmer, B. Wiestler, and B. H. Menze, "BraTS Toolkit: Translating BraTS Brain Tumor Segmentation Algorithms Into Clinical and Scientific Practice," Frontiers in Neuroscience, vol. 14, Apr. 2020.
[34] L. Sun, L. Zhang, and D. Zhang, "Multi-Atlas Based Method in Brain MR Image Segmentation," Chinese Medical Sciences Journal, p. 88, 2019.
[35] B. Thyreau and Y. Taki, "Learning a cortical parcellation of the brain robust to the MRI segmentation with convolutional neural networks," Medical Image Analysis, vol. 61, p. 101639, Apr. 2020.
[36] S. Alqazzaz, X. Sun, X. Yang, and L. Nokes, "Automated brain tumor segmentation on multi-modal MR image using SegNet," Computational Visual Media, vol. 5, no. 2, pp. 209-219, Apr. 2019.
[37] L. Sun, S. Zhang, H. Chen, and L. Luo, "Brain Tumor Segmentation and Survival Prediction Using Multimodal MRI Scans With Deep Learning," Frontiers in Neuroscience, vol. 13, Aug. 2019.
[38] U. Baid, S. Talbar, S. Rane, S. Gupta, M. H. Thakur, A. Moiyadi, N. Sable, M. Akolkar, and A. Mahajan, "A Novel Approach for Fully Automatic Intra-Tumor Segmentation With 3D U-Net Architecture for Gliomas," Frontiers in Computational Neuroscience, vol. 14, Feb. 2020.
[39] S. Maharjan, A. Alsadoon, P. W. C. Prasad, T. Al-Dalain, and O. H. Alsadoon, "A novel enhanced softmax loss function for brain tumour detection using deep learning," Journal of Neuroscience Methods, vol. 330, p. 108520, Jan. 2020.
[40] D. Ataloglou, A. Dimou, D. Zarpalas, and P. Daras, "Fast and Precise Hippocampus Segmentation Through Deep Convolutional Neural Network Ensembles and Transfer Learning," Neuroinformatics, vol. 17, no. 4, pp. 563-582, Mar. 2019.
[41] S. Vidyasagar and A. Sulaiman F, "Evaluation of Primary Brain Tumor with Magnetic Resonance Imaging," International Journal of Contemporary Medicine, Surgery and Radiology, vol. 4, no. 1, Jan. 2019.
[42] L. BRAIN, "Isolation of Nuclei from Adult Human Brain Tissue for 10x Genomics Platform v1 (protocols.io.y6rfzd6)," protocols.io, Mar. 2019.
[43] B. Song, H. Wang, and R. Wei, "Brain Tumor Segmentation of Magnetic Resonance Imaging Based on Improved Support Vector Machines," Journal of Medical Imaging and Health Informatics, vol. 9, no. 5, pp. 1011-1016, Jun. 2019.
[44] P. Prasanna, A. Karnawat, M. Ismail, and A. Madabhushi, "Radiomics-based convolutional neural network for brain tumor segmentation on multiparametric magnetic resonance imaging," Journal of Medical Imaging, vol. 6, no. 02, p. 1, May 2019.
[45] H. Chen, Z. Qin, Y. Ding, L. Tian, and Z. Qin, "Brain tumor segmentation with deep convolutional symmetric neural network," Neurocomputing, vol. 392, pp. 305-313, Jun. 2020.
[46] TCGA-LGG - the cancer imaging archive (TCIA) public access - cancer imaging archive wiki [Online]. Available, https://wiki.cancerimagingarchive.net/display/Public/TCGA-LGG.
[47] J. Li, J. Zheng, M. Ding, and H. Yu, "Multi-branch sharing network for real-time 3D brain tumor segmentation," Journal of Real-Time Image Processing, Jan. 2021.
[48] F. Chollet, "Vgg16_weights." [Online]. Available: https://github.com/fchollet/ deeplearningmodels/releases/download/v0.1/vgg16_weights_tf_dim_ordering_tf_kernels_notop.h5.
[49] brain-segmentation-pytorch | Kaggle. [Online]. Available, https://www.kaggle. com/mateuszbuda/brain-segmentation-pytorch/data.
[50] G. M. Tarhini and R. Shbib, "Detection of Brain Tumor in MRI Images Using Watershed and Threshold-Based Segmentation," International Journal of Signal Processing Systems, vol. 8, no. 1, pp. 19-25, Mar. 2020.
[51] L. Zhao, Q. Li, C.-H. Wang, and Y.-C. Liao, "3D Brain Tumor Image Segmentation Integrating Cascaded Anisotropic Fully Convolutional Neural Network and Hybrid Level Set Method," Journal of Imaging Science and Technology, vol. 64, no. 4, pp. 40411-1-40411-10, Jul. 2020.
[52] J. Jeong, Y. Lei, S. Kahn, T. Liu, W. J. Curran, H.-K. Shu, H. Mao, and X. Yang, "Brain tumor segmentation using 3D Mask R-CNN for dynamic susceptibility contrast enhanced perfusion imaging," Physics in Medicine & Biology, vol. 65, no. 18, p. 185009, Sep. 2020.